Morocco Journal of Chemistry

Study of Pyrazolo[3,4-d] pyrimidine Derivative as Corrosion Inhibitor on 904L stainless Steel in Molar H_3PO_4

Maria. Boudalia[(a)*], Abdelkabir. Bellaouchou[(a)], Abdellah. Guenbour[(a)], Hind. Bourazmi[(a)], Mohammed. Tabiyaoui[(a)], Mohammed. El Fal[(b)*], Youssef. Ramli[(b),(c)], El Mokhtar Essassi[(b)], Hicham. Elmsellem[(d)]

[(a)]Laboratory of Materials, Nanotechnology and Environment, Faculty of Science, University of Mohamed-V- Av. Ibn Battouta, BP 1014 Agdal-Rabat, Morocco

[(b)]Laboratoire de Chimie Organique Hétérocyclique, URAC 21, Pôle de Compétences Pharmacochimie, Université Mohammed V-Agdal, Faculté des Sciences, Av. Ibn Battouta, BP 1014 Rabat, Morocco.

[(c)]Laboratoire Nationale de contrôle des medicaments,Direction du médicament et de pharmacie,Bp6206,10000 Rabat,Maroc

[(d)]Laboratoire de Chimie Appliquée et environnement (LCAE-URAC18), Faculté des Sciences, Université Mohammed Premier, Oujda, Morocco

**Corresponding author. E-mail : maria.boudalia@yahoo.com and elfal.mohammed@gmail.com*

Received 15 May 2014, Revised 04 June 2014, Accepted 06 June 2014.

Abstract

The corrosion inhibition of stainless steel type 904 L SS with different concentrations (10^{-3}-10^{-6} M) of 1,5-diallyl-1H-pyrazolo[3,4-d] pyrimidine (DPP) in acid solutions was investigated by potentiostatic polarization measurements. The effect of temperature (298-353°K) on corrosion parameters was examined. The open circuit potential values in the presence and absence of DPP noted before and after experiments indicated the formation of passive film on the surface of the samples. It was found that corrosion potential (E_{corr}) increases with increasing DPP concentrations, while, corrosion current (i_{corr}) decreases. Inhibition efficiency of DPP in 1M H_3PO_4 . The inhibitor functions through adsorption and follows languimir isotherm in the acid. Activation energy (E_a) for adsorption of DPP is calculated. The values of ΔG_{ads} decreased (attained more negative values) with increasing temperature.

Keywords: Corrosion, Stainless steel, DPP, EIS, languimir isotherm.

I/Introduction

Phosphoric acid solutions are widely used in chemical and several industrial processes such as acid pickling, acid cleaning, acid descaling and oil well acidizing, which require the use of corrosion inhibitors [1 -5].

Austenitic stainless steels (SS) are the commonly used construction materials, owing to their excellent resistance to general corrosion, high strength. However, they are susceptible to localized corrosion in the presence of aggressive. The use of inhibitors is one of the most practical methods of protecting against corrosion especially for materials in acid media; most of the well known acid inhibitors are organic compounds containing nitrogen, sulphur and oxygen atoms.

N-heterocyclic compounds are well qualified to play more protection for steel corrosion [6-8]. Many N-heterocyclic compounds such as derivatives of pyrazole [9-11], bipyrazole[12-14] triazole[15-17], tetrazole [18-20], imidazole[21-24], pyridine[25-28], pyrimidine[29] and pyridazine[30,31] have been reported as effective corrosion inhibitors for steel in acidic media. The heterocyclic compound containing nitrogen atoms can easily be protonated in acidic medium to exhibit good inhibitory action on the corrosion of metals in acid solutions. The present study aimed to test new compound named 1,5-diallyl-1H-pyrazol o[3,4-d]pyrimidin-4(5H)-one on the corrosion of stainless steel in 1M phosphoric acid solution. The study has been evaluated using potentiodynamic polarization and EIS techniques at various concentrations.

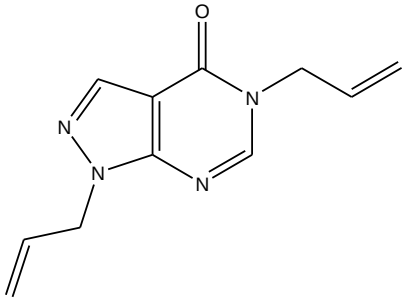

Fig1: 1,5-diallyl-1H-pyrazol o[3,4-d]pyrimidin-4(5H)-one

2/Experimental Procedure

2.1. Materials and reagents

Stainless steel type 904L samples were of the compositions (in wt.%): 0.0013% C, 1.45% Si, 1.84% Mn, 25.09% Ni, 20.77% Cr, 0.029% P, 43.97% Fe . The stainless steel sheet of 0.75 cm^2 area was mechanically polished with different grades (400, 800, 1200, and 1400) of emery papers in sequence. After polishing the specimens were washed with double distilled water and were used as working electrode for the test solution. A saturated calomel electrode (SCE) was used as reference electrode and a platinum plate as the counter electrode. The solutions were prepared with addition of different concentrations ((10^{-3}-10^{-6} M) of DPP in acid solutions (H_3PO_4). Potentiodynamic studies were performed by a potentiostate Prior to polarization measurement.Experiments were carried out at different temperatures (283-353°K) controlled by a thermostat. The anodic and cathodic polarization curves were obtained at a scan rate of $2mVs^{-1}$.

The experimental apparatus used for electrochemical studies is the PGZ 100 potentiostat , monitored by a PC computer and Voltamaster 4.0 software. .

The electrochemical impedance spectroscopy (EIS) were conducted in the frequency range of 100 kHz-100 mHz, with an amplitude signal of 10 mV peak to peak, The impedance diagrams are given in the Nyquist representation. To study the effect of temperature, the cell was immersed in water thermostat in the temperature range of 298–353°K.During each experiment, the test solution was mixed with a magnetic stirrer.

2.2. Synthesis

To a solution of 1H-pyrazolo[3,4-d]pyrimidin-4(5H)-one (0.5 g, 3.67 mmol) dissolved in DMF (30 ml) was added 3-bromoprop-1-ene (1.4 ml, 7.4 mmol), potassium carbonate (1.02g , 7.4 mmol) and a catalytic amount of tetra-n-butylammonium bromide (0.1 g, 0.4 mmol). The mixture was stirred for 48 h and the reaction monitored by thin layer chromatography. The mixture was filtered and the solvent removed under vacuum. After evaporation of the solvent under reduced pressure, the residue obtained was chromatographed on silica

column (hexane/ ethyl acetate 4:6 v/v). Recrystallization occurred in the same eluent. The product obtained was characterized by ^{1}H NMR, ^{13}C, IR and mass.

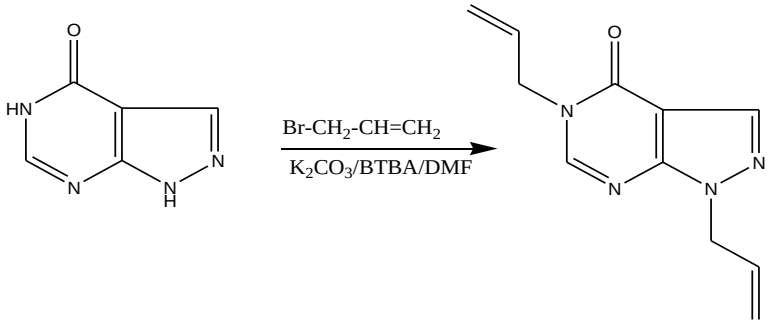

Characterization of 1,5-diallyl-1H-pyrazolo[3,4-d]pyrimidin-4(5H)-one. Light yellow solid (56 % yield), **^{1}H NMR (DMSOd$_6$):** δ 4.59 (dd, 2H, N_5CH_2,^{3}J=4.59, ^{4}J=4.57Hz), 4.89 (dd, 2H, N_1CH_2, ^{3}J=4.9, ^{4}J=4.68Hz), 4.94 (m, 2H, =CH_2, ^{3}J=4.9, ^{4}J=4.6), 5.1 (m, 2H, =CH_2, ^{3}J=5.1, ^{4}J=4.8), 5.95 (m, 1H, =CH, ^{3}J=5.93 ,^{4}J=5.63), 6.02 (m, 1H, =CH, ^{3}J=5.91, ^{4}J=5.71Hz), 8.10 (s, 1H, H-3), 8.34 (s, 1H, H-6).

^{13}C NMR (DMSO-d6): δ 47.46 (N_5-CH_2), 49.56 (N_1-CH_2), 105.46 (C, C-3a), 117.79 (=CH_2), 118.02 (=CH_2), 133.88 (=CH_2), 135.08 (CH, C-3), 151.06 (CH, C-6), 151.62 (C, C-7a), 156.60 (CO, C-4). HRMS (APPI) calcd for $C_{11}H_{12}N_4O$ $(M + H)^+$ m/z: 217.11.

3/Results and Discussion

3.1 Potentiodynamic response

The Fig 2 show that the polarization curves for stainless steel 904L with and without various concentrations of DPP at 298° K. the addition of this inhibitor hindered the acid attack on the stainless steel electrode and a comparison of curves of the cases with respect to the blank sample, revealed that increasing concentration of the inhibitor gives rise to a consistent decrease in anodic and cathodic current densities and the corrosion potential (E_{corr}) shifts to - ve direction, indicating the inhibitor to be of anodic in character and the formation of a surface film [32].

The corrosion current densities (i_{corr}) were obtained by extrapolation of the Tafel lines. The variations of the inhibition efficiency (%E) was calculated by using the following formula, here i^0_{corr} and i_{corr} are the corrosion current densities in the absence and presence of the inhibitor, respectively:

$$E = \left(1 - \frac{i_{corr}}{i^{\circ}_{corr}}\right) * 100 \qquad (1)$$

The current density (i_{corr}), corrosion potential (E_{corr}), and calculated inhibition efficiencies (%E) are listed in Tables 1.

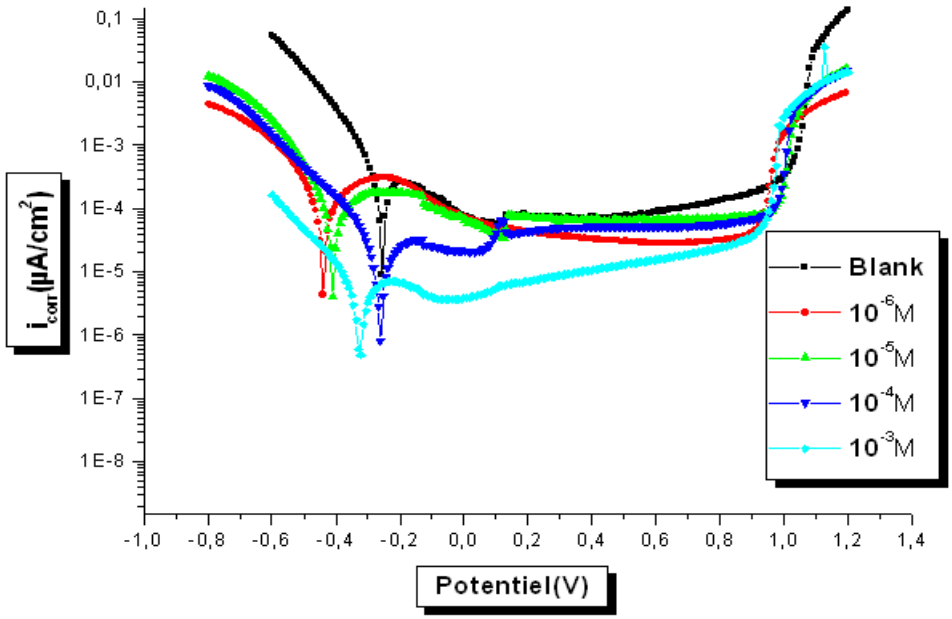

Fig2: Polarization curves of stainless steel in 1M H_3PO_4 containing different concentrations of DPP

Table1. Electrochemical parameters of stainless steel in 1M H_3PO_4 in the presence of different concentrations of DPP at 298°K

Alloy	Blank	10^{-6}	10^{-5}	10^{-4}	10^{-3}
i_{corr}(A.cm^{-2})	*3.10 10^{-4}*	*1.65 10^{-4}*	*4.6610^{-5}*	*2.61 10^{-5}*	*1.0910^{-5}*
E_{corr}($mV/_{Ag/AgCl}$)	*-242.6*	-439.8	63 ,3	-9,2	-43,1
Ba	1050	983.1	476.8	783.6	1178
Bc	-141.4	-206.4	-126.5	-160.8	-196.6
E%	-	74	86.4	91.6	97.6

The data in Table 1 show that increasing compound concentrations slightly shifts the values of corrosion potential (E_{corr}) in a cathodic direction indicating that they act as mixed-type inhibitors. The cathodic Tafel slope (β_c) shows a change with the addition of DPP, which suggests that the inhibiting action occurred by simple blocking of the available cathodic sites on the metal surface, which led to a decrease in the exposed area necessary for hydrogen evolution and lowered the dissolution rate with increasing inhibitor concentration.

In the anodic domain, the presence of DPP decreases anodic current density, the highest effect is observed with these product increase of the over voltage near the corrosion potential

Table 1 clearly indicates a decrease in the corrosion rate (CR) in the presence of DPP. This effect is hugely marked at higher concentrations of inhibitors. The inhibitive action is more explicit using E% data which increases with inhibitor concentration to reach 97.6% for DPP at 10^{-3}M.

The inhibitor studied inhibited the corrosion of stainless steel in 1M H_3PO_4, The high values of E% observed in our case may be explained by the presence of nitrogen atoms, π-electron of pyrazolo[3.4-d]pyrimidine . The nitrogen atoms are the major adsorption centers for their interaction with the metal surface [33].

3.2. Electrochemical Impedance Spectroscopy (EIS)

The corrosion behavior of stainless steel, in 1M H_3PO_4 solution with and without inhibitor, was also investigated by electrochemical impedance spectroscopy (EIS) measurements at 398°K after 80 min of immersion. Fig.3 showed impedance behavior of stainless steel corrosion in the form of Nyquist plots.

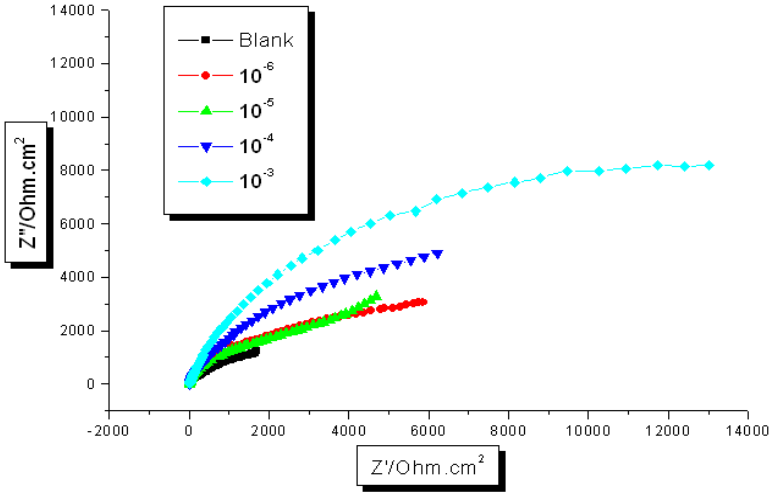

Fig3. Nyquist diagrams 904L stainless steel in 1M H_3PO_4 without and with different concentrations of DPP.

The impedance parameters derived from these plots are given in Table 2. Double layer capacitance values (C_{dl}) and charge-transfer resistance values (R_{ct}) were obtained from impedance measurements. In the case of the electrochemical impedance spectroscopy, E (%) is calculated by charge transfer resistance according to the relation:

$$E\% = \frac{R_{ct(inh)} - R_{ct}}{R_{ct(inh)}} * 100 \qquad (2)$$

Table 2 . Impedance parameters of 904L stainless steel in 1 M H_3PO_4 different concentrations of DPP compounds

	Blank	10^{-3}	10^{-4}	10^{-5}	10^{-6}
R_T (Ω cm^2)	107.2	887.4	680	502	454
C_{dl} (μF cm^{-2})	180.9	70.5	99.5	54.6	74, 5
% E	-	87.9	84.2	78.6	76.3

Where $Rct_{(inh)}$ and R_{ct} are the charge transfer resistance in the presence and absence of pyridazine, respectively For Nyquist plots (Fig 3) it is clear that the impedance diagrams contain a semi-circular appearance. The size of the semicircle increases with the inhibitor concentration, indicating the charge transfer process as the main controlling factor of the corrosion of 904L stainless steel. It is apparent from the plot that the impedance of the inhibited solution has increased with the increase in the concentration of the inhibitors [34]. The experimental result of EIS measurements for the corrosion of 904L stainless steel in 1 M H_3PO_4 in the absence and presence of inhibitors is given in Table 2. As it can be observed from the table, the charge-transfer resistance values (R_{ct}) increased with increase in the concentration of the inhibitor whereas values of the capacitance of the interface

(C_{dl}) starts decreasing, with increase in inhibitor concentration, which is most probably due to the decrease in local dielectric constant and/or increase in thickness of the electrical double layer. This suggests that the inhibitor acts via adsorption at the metal/solution interface [34,35] and the decrease in the C_{dl} values is caused by the gradual replacement of water molecules by the adsorption of the inhibitor molecules on the electrode surface, which decreases the extent of metal dissolution [36]. The inhibiting effectiveness increases with the concentration of the inhibitors to reach a maximum value from 87.9%.

3.3. Effect of temperature

The effect of temperature on cathodic and anodic polarization curves for the 904L stainless steel is shown in Fig 5. The results of these curves revealed that corrosion current density (i_{corr}) increases with increasing temperature, so that highest current density (i_{corr}) values were observed at 298°C-353°C while corrosion potential (E_{corr}), decreased with increasing temperature. This proves that the inhibition occurs through the adsorption of the inhibitor on the surface.

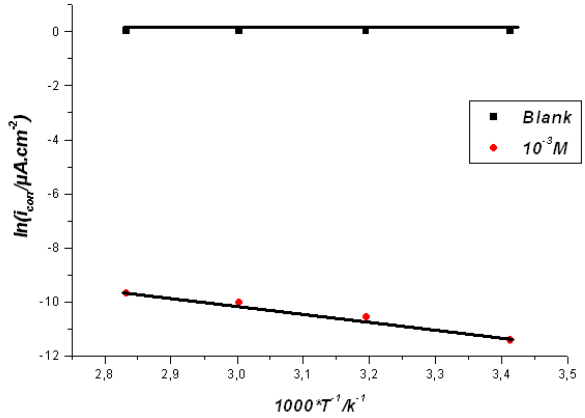

Fig4. Arrhenius straight lines calculated from corrosion rate of stainless steel in 1M H_3PO_4 and 1 M H_3PO_4+ 10^{-3}M DPP

The activation energy of the corrosion process can be calculated using the following equation:

$k = A\exp(-E_a/RT)$ (3).

Where E_a is the activation energy A is the frequency factor, T is the absolute temperature, R is the gas constant and k is the rate of metal dissolution reaction and is directly related to corrosion current density (i_{corr}) [37, 38]. Plotting $\ln(i_{corr})$ versus 1/T ,The value of E_a can be calculated from the slopes of straight lines (Fig). The value of E_a is 25.28kJ mol^{-1} for blank sample and 17.7kJmol^{-1} for inhibitor at 10^{-3}M of inhibitor in phosphoric acid solutions respectively.

The activation energy is higher in the presence of inhibitor than in the absence of inhibitor while this result is attributed to its physical adsorption [34, 39-40]. This type of inhibitor retards the corrosion process at 298°K and the inhibition is considerably decreased at elevated temperature.

Table.3 the influence of temperature on the electrochemical parameters for stainless steel electrode immersed in 1M H_3PO_4 and in 1M H_3PO_4+ 10^{-3}M [DPP]

	1M H_3PO_4		10^{-3}M+1M H_3PO_4		%E
	E_{corr}(mV/SCE)	I_{corr}(µA /cm^2)	E_{corr}(mV/SCE)	I_{corr}(µA /cm^2)	
293°K	*242.6*	*310*	-259.8	10.9	96.4
313°K	*116.8*	*550*	-357	39	92.9
333°K	*157.7*	*625*	-309.4	58	90.3
353°K	*160.1*	*630*	-422.7	60	90.4

3.4 Application of adsorption isotherm

It is well recognised that the first step in inhibition of metallic corrosion is the adsorption of organic inhibitor molecules at the metal/solution interface and that the adsorption depends on the molecule's chemical composition, the temperature and the electrochemical potential at the metal/solution interface. In fact, the solvent H_2O molecules could also adsorb at metal/solution interface. So the adsorption of organic inhibitor molecules from the aqueous solution can be regarded as a quasi-substitution process between the organic compounds in the aqueous phase [Org(sol)] and water molecules at the electrode surface [$H_2O_{(ads)}$] [41].:

$$Org_{sol} + nH_2O_{ads} \longrightarrow Org_{ads} + nH_2O_{sol} \quad (4)$$

Where (n) is the size ratio, that is, the number of water molecules replaced by one organic inhibitor. Basic information on the interaction between the inhibitor and the steel surface can be provided by the adsorption isotherm. In order to obtain the isotherm, the linear relation between degree of surface coverage (Θ) values (Θ = E%/100; Table 4) and inhibitor concentration (C_{inh}) must be found. Attempts were made to fit the Θ values to various isotherms including Langmuir, Temkin Frumkin and Flory–Huggins. By far the best fit is obtained with the Langmuir isotherm. This model has also been used for other inhibitor systems [42, 43]. According to this isotherm, Θ is related to C_{inh} by:

$$\frac{C}{\theta} = \frac{1}{K} + C \quad (5)$$

Where K_{ads} denotes the equilibrium constant for the adsorption process.

Fig.5 shows the plots of C_{inh}/Θ versus C_{inh} and the expected linear relationship is obtained for all compounds. The strong correlations (R^2 = 0.99984 confirm the validity of this approach.

The values of K_{ads} obtained from the Langmuir adsorption isotherm are listed in Table 4, together with the values of the Gibbs free energy of adsorption calculated from the equation ΔG°_{ads}= - RTLn (55.5K_{ads})

Where R is the universal gas constant, T the thermodynamic temperature and the value of 55.5 is the concentration of water in the solution [44].

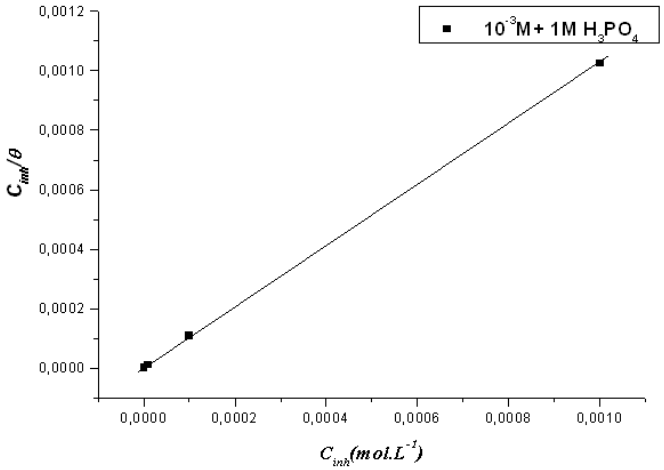

Fig 5. Langmuir adsorption isotherm plot for the adsorption of the used inhibitor on phosphoric acid medium

The value K_{ads} calculated from the reciprocal of intercept of isotherm line is indicating in the Table 4. The high value of the adsorption equilibrium constant reflects the high adsorption ability of this inhibitor on 904L stainless steel surface.

From Eq. (6), ΔG°_{ads} was calculated as -37.35 kJ mol^{-1} for DPP. The negative value of standard free energy of adsorption indicates spontaneous adsorption of our molecule on 904L stainless steel surface and also the strong interaction between inhibitor molecule and the metal surface [45, 46]. Generally, the standard free energy values of - 20 kJ mol^{-1} or less negative are associated with an electrostatic interaction between charged molecules and charged metal surface (physical adsorption); those of - 40 kJ mol^{-1} or more negative involves charge sharing or transfer from the inhibitor molecules to the metal surface to form a co-ordinate covalent bond (chemical adsorption) [47,48].The value of ΔG°_{ads} in our measurement is -37.35 kJ mol^{-1} for it is suggested that the adsorption involves the physisorption interactions.

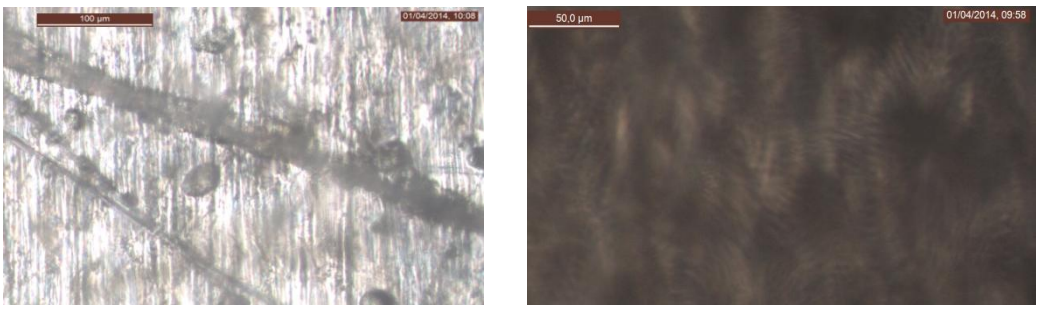

Fig6. Examination by electron microscopy of the surface of the 904 L stainless steel in phosphoric acid (a): 1M H3PO4 without addition of inhibitor ; (b): 1M H3PO4 + 10-3M of DPP

3.5 Quantum chemical calculations

The quantum theoretical calculations were carried out with the Gaussian 03 program package [49]. The complete geometry optimization of the pyrimidine derivatives as corrosion inhibitor was carried out at DFT (Density Functional Theory) using the hybrid functional B3LYP level taking into account the exchange and the correlation with Beck's three parameters exchange functional along with Lee [50,51] non-local correlation

functional. All Calculations of DFT/B3LYP theory were done using 6-31G (d,p) basis set. The following quantum chemical indices were considered: the energy of the highest occupied molecular orbital (E_{HOMO}), the energy of the lowest unoccupied molecular orbital (E_{LUMO}), $\Delta E = E_{LUMO} - E_{HOMO}$, the dipole moment (μ) and total energy. Fig.7 shows full geometry optimization of the inhibitor molecule. The equilibrium geometry structures and the frontier molecule orbital density distributions of the molecule are shown in Fig. 8 , and the quantum chemical parameters are listed in Table 5.

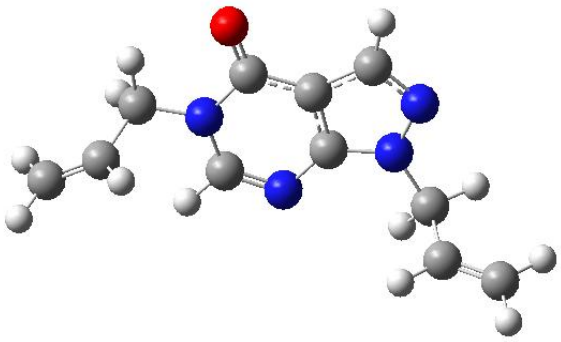

Fig.7. Optimized structures of 1,5-diallyl-1H-pyrazolo[3,4-d] pyrimidine (DPP).

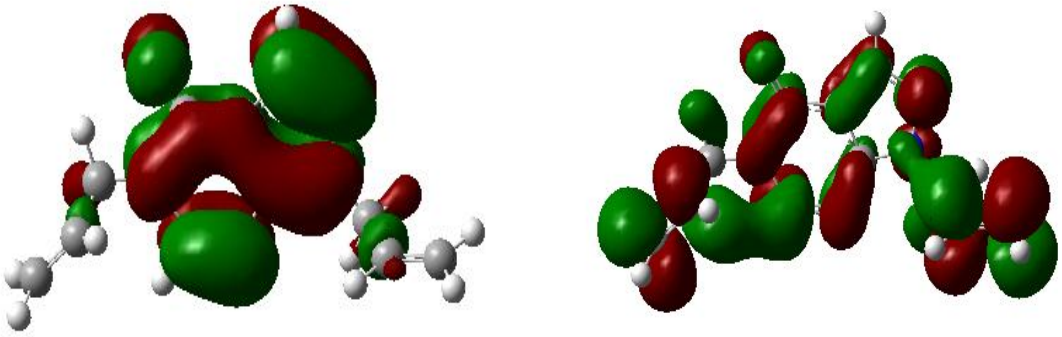

HOMO **LUMO**

Fig.8 The frontier molecular orbital density distribution of 1,5-diallyl-1H-pyrazolo[3,4-d] pyrimidine (DPP)

Analysis of Fig. 8 shows that the distribution of two energies HOMO and LUMO, we can see that the electron density of the HOMO and LUMO location was distributed almost of the entire molecule.

Mulliken charges of the atoms in inhibitor molecule are also shown in Table.4. The larger negative charge of the N atom, the better is the action as an electron donor.

By careful examination of the values of Mulliken charges, the larger negative N atoms of DPP, which could donate its lone pair electron to the unfilled orbital of the metal atom, the DPP derivative molecule can be adsorbed on the metal surface [52].

Table 4. Mulliken charge density data of DPP.

DPP	
1 N -0.286158	9 C -0.084545
2 C 0.086218	10 O -0.344603
3 N -0.188616	11 C -0.014829
4 C 0.050072	12 C -0.195277
5 C -0.289665	13 C -0.202559
6 C 0.387167	14 C 0.026008
7 N -0.102389	15 C -0.193222
8 N -0.070975	16 C -0.187607

E_{HOMO} is often associated with the capacity of a molecule to donate electron. High value of E_{HOMO} probably indicates a tendency of the molecule to donate electrons to appropriate acceptor molecules with low energy and empty molecular orbital. E_{LUMO} indicates the ability of the molecule to accept electrons. The lower the value of E_{LUMO}, the more probable is that the molecule would accept electrons [53-54]. According to frontier orbital theory, the reaction of reactants mainly occurs on HOMO and LUMO [55].

So, the smaller gap (ΔE) between E_{HOMO} and E_{LUMO} is the more probable to donate and accept electrons. The values of ΔE in Table 5, suggesting the strongest ability of the synthesized inhibitor to form coordinate bonds with d-orbitals of metal through donating and accepting electrons, is in good agreement with the experimental results. Additionally, for the dipole moment (μ), higher value of μ will favor the enhancement of corrosion inhibition [56-57]. From Table 5, the value of μ is higher, which is also in agreement with the experimental results mentioned above.

Table.5. Calculated quantum chemical parameters of the studied compound.

Quantum parameters	
E_{HOMO} (eV)	-0.306
E_{LUMO} (eV)	-0.165
ΔEgap (eV)	0.141
μ (debye)	4.0404
TE (u.a.)	0.16682493

The synthesized inhibitor shows the highest inhibition efficiency because it has the highest HOMO energy and this reflects the greatest ability (the lowest ΔE) of offering electrons. It can be seen from Table 5 that the ability of the synthesized inhibitor to donate electrons to the metal surface, which is in good agreement with the higher inhibition efficiency of the synthesized inhibitor.

Conclusion :

- Polarization study shows that compounds act as mixed-type inhibitors.
- Impedance method indicates that compounds adsorbs on 904L stainless steel surface with increasing

charge transfer resistance and decreasing the double-layer capacitance.

- the examined pyrimidine derivative is effective corrosion inhibitors for 904 L stainless steel in 1M H_3PO_4 solution.
- The inhibition efficiency was found to increase by increasing the inhibitor concentrations and with decreasing temperature.
- The negative values of $\Delta G°_{ads}$ indicate that the adsorption of the inhibitors molecule is a spontaneous process and an adsorption mechanism is typical of physisorption.
- The inhibition efficiency decreased with increasing temperature as a result of the higher dissolution of stainless steel at higher temperature.
- Quantum chemical approach is adequately sufficient to also forecast the inhibitor effectiveness using the theoretical approach. However, it may be used to find the optimal group of parameters that might predict the structure and molecule suitability to be an inhibitor.

References

[1]. M. Batros and N. Hakerman, *J. Electrochem. Soc.,* 139 (1992) 3429.

[2]. F. Bentiss, M. Lagrenee, M. Traisnel, B. Mernari, and H. El Attari, *J. Appl. Electrochem.*, 29 (1999). 1073.

[3]. P. Kutej, J. Vosta, J. Pancir, J. Macak, and N. Hackerman, *J. Electrochem. Soc*., 142 (1995) 829.

[4]. M. Dahmani, A. Et-Touhami, S.S. Al-Deyab, B. Hammouti and A. Bouyanzer, *Int. J. Electrochem. Sci.*, 5 (2010) 1060.

[5]. J.M. Bastidas, J.L. Polo and E. Cano, *J. Electrochem. Soc*., 30 (2000) 1173.

[6]. M. Boudalia,A. Guenbour,A. Bellaouchou,R. M. Fernandez-Domene,and J. Garcia-Anton*al J.* Inter Journal of Corros., 2013 (2013)9.

[7]. E.E. Foad El Sherbini, *Mater. Chem. Phys.,* 60 (1999) 286.

[8]. W.W. Frenier, F.B. Growcock and V.R. Lopp, *Corrosion.*, 44 (1988) 590.

[9]. M.A. Quraishi and D. Jamal, *Corrosion.*, 56 (2000) 156.

[10]. M. Benabdellah, A. Yahyi, A. Dafali, A. Aouniti, B. Hammouti and A. Ettouhami, *Arab. J. Chem.*, 4 (2011) 343.

[11]. M. Elayyachy, B. Hammouti, A. El Idrissi and A. Aouniti, *Port. Electrochim. Acta*., 29 (2011) 57.

[12]. J.M. Sykes, *Br. Corros. J.*, 25 (1990) 175.

[13]. P. Chatterjee, M.K. Banerjee and K.P. Mukherjee, *Indian J. Technol.*, 29 (1991) 191.

[14]. J.M. Bockris, and B. Yang, *J. Electrochem. Soc*., 138 (1991) 2237.

[15]. A. Zarrouk, I. Warad, B. Hammouti, A Dafali, S.S. Al-Deyab and N. Benchat, *Int. J. Electrochem. Sci.*, 5 (2010) 1516.

[16]. DA. Vermilyea, in, First International Congress; Metal Corrosion; Butterworths; London; 1962, p 62

[17]. F. Bentiss, M. Traisnel, N. Chaibi, B. Mernari, H. Vezin and M. Lagrenee, *Corros. Sci.,* 44 (2002) 2271

[18]. I.El Ouali, B. Hammouti, A. Aouniti, Y. Ramli, M. Azougagh, E.M., Essassi and M. Bouachrine, *J. Mater. Environ. Sci.,* 1 (2010) 1.
[19]. K.F. Khaled, N.S. Abdelshafi, A. El-Maghraby and N. Al-Mobarak, *J. Mater. Environ. Sci.,* 2 (2011) 166.
[20]. J. Uhrea and K. Aramaki, *J. Electrochem. Soc*., 138 (1991) 3245.
[21]. S. Kertit and B. Hammouti, *Appl. Surf. Sci.,* 93 (1996) 59.
[22]. A.Chetouani, B. Hammouti, A. Aouniti, N. Benchat and T. Benhadda, *Prog. Org. Coat.,* 45 (2002) 373.
[23]. K. Bekkouch, A. Aouniti, B. Hammouti, S. Kertit, *J. Chim. Phys.,* 96 (1999) 838.
[24]. S. Kertit, B. Hammouti, M. Taleb and M.; Brighli, *Bull. Electrochem.,* 13 (1997) 241.
[25]. M. Bouklah, N. Benchat, A. Aouniti, B. Hammouti, M. Benkaddour, M. Lagrenee, H. Vezin and F. Bentiss, *Prog. Org. Coat.,* 51 (2004) 118.
[26]. L. Wang, *Corros. Sci.,* 48 (2006) 608.
[27]. M. Lagrenee, B. Mernari, N. Chaibi, M. Traisnel, H. Vezin and F. Bentiss, *Corros. Sci.,* 43 (2001) 951.
[28]. S. Rengamani, S. Muralidharan, M. Anbu Kulandainathan and S. Venkatakrishna Iyer, *J. Electrochem. Soc*., 24 (1994) 355.
[29]. F. Bentiss, F. Gassama, D. Barbry, L. Gengembre, H. Vezin, M. Lagrenee, M. Traisnel, *Appl. Surf. .Sci.,* 252 (2006) 2684.
[30]. H. Zarrok, R. Saddik, H. Oudda, B. Hammouti, A. El Midaoui, A. Zarrouk, N. Benchat, M. Ebn Touhami, *Der Pharma Chemica*., 3 (2011) 272.
[31]. A.Chetouani, B. Hammouti, A. Aouniti, N. Benchat, T. Benhadda, *Prog. Org. Coat.,* 45 (2003) 73.
[32]. S.M.A.Hosseini & S.Z.Tajbakhsh.*Phy Chem.*,1(2007)55.
[33].S. Zhang, Z. Tao, W. Li, B. Hou, *Appl. Surf. Sci*., 255 (2009) 6757
[34].M. Boudalia, A. Guenbour, A. Bellaouchou, A. Laqhaili, M. Mousaddak, A. Hakiki, B.Hammouti, E.E. Ebenso. *Int. J. Electrochem.* Sci.,8 (2013)7414 – 7424.
[35].T. Tsuru, S. Haruyama, B. Gijutsu, *J. Jpn. Soc. Corros. Eng.,* 27 (1978) 573.
[36]. K. F. Khaled, *Electrochim. Acta*., 48 (2003) 2493.
[37]. K.Gomma Gamal.Mater Chem Phys.,131(1998)55.
[38]. O.L.Riggs & R.M.Hurd,Corrosion.,252(1967)33.
[39].M.Abdellah,Corro Sci.,717(2002) 44.
[40]. I.K.Putiolova,S.A.Balezin,*Metallic Corrosion Inhibitors(*Pergamon Press,Oxoford).,1960,30.
[41]. N.M. Guan, L. Xueming, L. Fei, Mater. Chem. Phys., 86 (2004) 59.
[42]. M. Sahin, S. Bilgic, H. Yılmaz, Appl. Surf. Sci., 195 (2002) 1-7.
[43]. M. Kissi, M. Bouklah, B. Hammouti, M. Benkaddour, Appl. Surf. Sci., 252 (2006) 4190-4197.
[44]. E. Machnikova, K. H. Whitmire, N. Hackerman, Electrochim. Acta., 53 (2008) 6024-6032
[45]. O. Olivares, N. V. Likhanova, B. Gomez, J. Navarrete, M.E. Llanos-Serrano, E. Arce, J. M. Hallen, Appl. Surf. Sci., 252 (2006) 2894-2909.
[46]. G. Avci, Mater. Chem. Phys., 112 (2008) 234.

[47]. E. Bayol, A.A. Gurten, M. Dursun, K. Kayakırılmaz, Acta Phys. Chim. Sin., 24 (2008) 2236.

[48]. O.K. Abiola, N.C. Oforka , Mater. Chem. Phys., 83 (2004) 315.

[49]. M.J. Frisch, G.W. Trucks, H.B. Schlegel, G.E. Scuseria, M.A. Robb, J.R. Cheeseman, J.A. Montgomery Jr., T. Vreven, K.N. Kudin, J.C. Burant, J.M. Millam, S.S. Iyengar, Barone, B. Mennucci, M. Cossi, G. Scalmani, N. Rega, G.A. Petersson, H. Nakatsuji, M. Hada, M. Ehara, K. Toyota, R. Fukuda, J. Hasegawa, M. Ishida, T. Nakajima, Y. Honda, O. Kitao, H. Nakai, M. Klene, X. Li, J.E. Knox, H.P. Hratchian, J.B. Cross, C. Adamo, J. Jaramillo, S. Clifford, J. Cioslowski, B.B. Stefanov, G. Liu, A. Liashenko, P. Piskorz, I. Komaromi, R.L. Martin, D.J. Fox, T. Keith, M.A. Al-Laham, C.Y. Peng, A. Nanayakkara, M. Challacombe, P.M.W. Gill, B. Johnson, W. Chen, M.W. Wong, C. Gonzalez, J.A. Pople, Gaussian 03, Revision B.01, Gaussian Inc., Pittsburgh, PA, 2003.

[50]. Z. El Adnani, M. Mcharfi, M. Sfaira, M. Benzakour, A.T. Benjelloun, M. Ebn Touhami, Corros. Sci., 68 (2013) 223–230.

[51]. C. Lee, W. Yang, R.G. Parr, Phys. Rev., B 37 (1988) 785–789.

[52]. D.K.Yadav, B. Maiti, M.A. Quraishi, *Corrosion Science* .,52 (2010) 3586–3598

[53]. D. Ben Hmamou, R. Salghi, A. Zarrouk, H. Zarrok, B. Hammouti, S. S. Al-Deyab, El Assyry, N. Benchat, M. Bouachrine. Int. J. Electrochem. Sci., 8 (2013) 11526 - 11545

[54] .M.M. Ibrahim, M.A. Amin, K. Ichikawa , J. Mol. Struct., 985 (2011) 191.

[55]. N. Khalil, Electrochim. Acta., 48 (2003) 2635.

[56]. J. Zhang, J. Liu, W. Yu, Y. Yan, L. You, L. Liu, Corros. Sci., 52 (2010) 2059.

[57]. A. Anejjar, A. Zarrouk , R. Salghi , D. Ben Hmamou, H. Zarrok, S. S. Al-Deyab, M. Bouachrine, B. Hammouti, N. Benchat. Int. J. Electrochem. Sci., 8 (2013) 5961 - 5979